Effects of Flow on the Collapse Behavior of Polyelectrolyte Brushes in Poor Solvents

J. L. Harden[†]

Groupe de Dynamique des Phases Condensées, Unité Mixte de Recherche CNRS/Université Montpellier II no 5581, Case 026, Université Montpellier II, F-34095 Montpellier Cedex 5, France

Received December 17, 1996; Revised Manuscript Received June 12, 1997[⊗]

ABSTRACT: This paper examines the effects of flow on the collapse behavior of grafted polyelectrolyte layers in uniform permeation flows of poor solvent within a model based on the Alexander−deGennes ansatz that all chains behave alike in flow. This model accounts for both the polymer−solvent drag forces and the possible effects of solvent drag forces on the counterions within in the brush. The phase behavior of charged brushes under flow is examined in the limits of low and moderate charge per unit grafting area. In both limits, it is found that the first-order nature of the stretch−collapse transition occurring for Alexander−deGennes polyelectrolyte brushes in quiescent poor solvents also remains in the presence of solvent flow. However, there is a significant shift in the location of the first-order transition line and the second-order critical point as a function of solvent flow rate. In particular, the flow generally shifts the critical point and transition line toward smaller polyelectrolyte charge for flows out of the brush and toward larger polyelectrolyte charge for flows into the brush. As well as modifying the location of the transition, solvent flow also changes the susceptibility of the brush: the discontinuity in brush thickness across the transition line is a rapidly increasing function of solvent flow rate. Possible modifications due to structural inhomogeneities are briefly discussed.

1. Introduction

The properties of polymer brushes (polymers grafted by one end to a surface at high density) have been the subject of extensive experimental and theoretical investigation during the past 2 decades. The equilibrium properties of neutral polymer brushes are now well understood.[1−3] Recently, there has also been substantial progress toward understanding the equilibrium properties and structure of polyelectrolyte brushes (densely grafted layers of charged polymers). For a very recent review of polyelectrolytes in solution, see ref 4. Due to the solubility of charged polymers in polar solvents, polyelectrolyte brushes are of particular interest for applications in the stabilization of colloidal particles in aqueous solutions, for the modification of interface and membrane properties in aqueous environments, and for bioengineering and biomedical applications.

Under good and Θ-solvent conditions, chains grafted at sufficiently high density are highly extended, leading to a brush thickness which scales linearly with the degree of polymerization N of the chains. For the case of polyelectrolyte brushes, the grafted chains are more strongly stretched than neutral grafted chains at the same grafting density and solvent quality for the uncharged monomers.[5−10] In the charge-dominated regime, there is roughly one charge per correlation blob,[7] leading to a brush thickness which scales as $H \sim \alpha^{1/2}Na$ under Θ-solvent conditions,[7] and $H \sim \alpha^{2/5}Na$ under good solvent conditions,[9] where α is the fraction of charged monomers per chain and where a is the effective monomer size. These scaling predictions are consistent with the results of more detailed calculations, which give the monomer density profile within the brush as a function of α.[5,6,8,10] In particular, self-consistent field (SCF) calculations predict parabolic density profiles for neutral brushes,[11−13] while for polyelectrolyte brushes such approaches predict that, with increasing α, the brush height increases substantially and the density profile shifts from a parabolic profile toward a profile of the Gaussian type.[5,6,8]

The behavior of polymer brushes in poor solvent conditions is a bit more complex, especially for the case of polyelectrolyte brushes. Most polyelectrolytes of practical importance have nonpolar, organic backbones and hence are only marginally soluble in polar solvents. Thus, the poor solvent limit is the most relevant one for applications. Whereas neutral polymer brushes are expected to collapse continuously with decreasing solvent quality,[14] the collapse behavior of polyelectrolyte brushes can be more dramatic. Models for polyelectrolyte brush behavior based on the Alexander−deGennes ansatz of a uniform step-function density profile within the brush[15,16] predict a first-order phase transition to a collapsed state with decreasing charge fraction α or decreasing solvent quality.[17,18] Recent studies using Monte Carlo methods and variational calculations also report a first-order stretch−collapse transition for laterally homogeneous polyelectrolyte brushes under poor solvent conditions.[19] However, there is also the possibility that this discontinuous but homogeneous collapse transition may be preempted by spatial density variations in a poor solvent polyelectrolyte brush. Theoretical studies of lateral density fluctuations in polyelectrolyte[20] and neutral polymer[21−24] brushes indicate that such brushes can become unstable toward lateral microphase separation in poor solvent conditions. Furthermore, it was shown in ref 20 that this lateral phase separation mechanism may also preempt the first-order stretch-collapse transition studied in refs 17−19. On the other hand, recent SCF calculations of the density profile normal to the grafting surface for a laterally homogeneous polyelectrolyte brush predict an internal two-phase structure in poor solvent conditions consisting of a dense phase near the grafting surface separated by a sharp interface from a dilute phase in the outer portion of the brush.[25] Subsequent analysis indicates that such a two-phase brush structure would

[†] Present address: Department of Chemical Engineering, Johns Hopkins University, Baltimore, MD 21218-2689.

[⊗] Abstract published in *Advance ACS Abstracts,* August 1, 1997.

S0024-9297(96)01856-6 CCC: $14.00

collapse continuously with decreasing solvent quality,[26] although the existence of such layer-wise mesophase brush structures is in contradiction with the results of ref.[19] This mechanism of mesophase formation (either lateral or layer-wise) is roughly analogous to the formation of mesophase structures in weakly-charged polyelectrolyte solutions and gels.[27,28] Since these effects are still not properly understood even for static equilibrium conditions, I shall set them to one side in this paper and consider only the homogeneous deformation behavior of brushes.

Recent studies have considered the properties of polymer brushes under nonequilibrium conditions. In particular, the response of grafted layers to solvent flows and to the frictional forces occurring during the relative motion of brush-bearing surfaces in contact has been investigated in some detail.[29−42] The response of such polymer layers to flows has important implications for the stability under flow of dispersions of colloidal particles with polymer coatings, for the lubrication properties of polymer-coated surfaces, and for the permeability characteristics of brush-bearing porous media. The limit of strong flows, in which there may be significant deformation of grafted layers, is of particular importance. Such strong flow conditions can give rise to novel and unexpected brush behavior. In the case of neutral polymer brushes subjected to shear flows of good solvent, there is experimental evidence that the brushes can swell in the direction normal to the grafting surface in response to sufficiently high shear-rate flows parallel to the grafting surface.[29,30] Theoretical models can predict such swelling phenomena for neutral brushes in good solvent conditions,[34−37] as well as shear-induced deswelling phenomena for polyelectrolyte brushes in good solvent shear flows[39,40] and for neutral brushes in poor solvent shear flows.[41]

The situation for polyelectrolyte brushes in flows of poor solvent is perhaps more subtle since, in addition to the mechanical response to flow exhibited by a brush, solvent flows might also influence the phase behavior of the brush, leading to a modified stretch−collapse transition. The purpose of this paper is to consider the effects of solvent flow on the nature of this transition for the particular case of salt-free Alexander−deGennes polyelectrolyte brushes in *permeation* flows of poor solvent. Such flows might occur, for instance, when polymers grafted to a permeable surface are subject to hydrodynamic pressure gradients normal to the polymer layer. This simplified flow geometry (uniform permeation flow through homogeneous grafted layers) is adopted in order to clearly illustrate some of the generic effects of flow on phase behavior and to provide a firm basis for future studies in more realistic flow conditions. I will briefly comment on more realistic flows through inhomogeneous brushes at the end of this paper.

2. Model

Consider a brush consisting of monodisperse, charged chains of degree of polymerization N grafted at dimensionless surface density $\sigma \simeq (a/\xi_0)^2$ to a flat porous medium under salt-free, poor solvent conditions and at high grafting densities $\sigma \gg N^{-1}$, where a is the Kuhn length and ξ_0 is the average distance between grafting points. It is assumed that a fraction α of the monomers are charged, e.g., negatively, and that the brush is subjected to a permeation flow of solvent with viscosity η and average macroscopic flow rate $\vec{V} = \pm V\hat{z}$ perpendicular to the grafting surface as sketched in Figure 1.

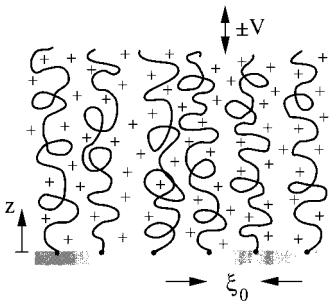

Figure 1. Sketch of a polyelectrolyte brush in a solvent permeation flow $V(z) = \pm V\hat{z}$ normal to the grafting surface.

For simplicity, I adopt the Alexander−deGennes-type ansatz that all chains behave alike. Note that this approximation is more reasonable for brushes subjected to external stretching forces than for undeformed brushes, in which strong fluctuations of the positions of free chain ends occur.[5−13] In principle, grafted chains in solvent flows generally deform nonuniformly.[42−43] However, it was shown in ref 42 that, at least for neutral brushes in permeation flows, the essential features of brush deformation under flow are recovered by adopting a "monoblock" view[43] of effectively uniform chain deformation. This is also expected to be true for polyelectrolyte brushes in poor solvent permeation flows, and so the monoblock ansatz will be adopted in this paper as well. Thus, the state of the brush may be characterized by its thickness H [or equivalently by the monomer volume fraction $\phi \simeq Na^3/(H\xi_0^2)$] and by the volume fraction ϕ_{co} of the free counterions.

In the absence of flow, the free energy per chain is the sum of four terms: an elastic term F_{el} accounting for the entropic penalty for chain deformation, an osmotic term F_{int} involving monomer−solvent interactions, a mixing term F_{ion} accounting for the entropy of mixing of the mobile counterions, and an electrostatic term F_{ch} accounting for Coulomb interactions. The elastic energy per chain, within the Gaussian elasticity approximation, is given by

$$\frac{F_{el}}{k_B T} = \frac{1}{2}\frac{H^2}{Na^2} \tag{1}$$

The monomer−solvent interactions may be approximated by a virial expansion in the monomer volume fraction, leading to an interaction energy F_{int} per chain of the form

$$\frac{F_{int}}{k_B T} = -\frac{1}{2}\mathrm{N}u\tau\phi + \frac{1}{6}Nw\phi^2 \tag{2}$$

where u and w are dimensionless second and third virial coefficients, and $\tau = (\Theta - T)/T$ is the reduced temperature shift *below* the Θ temperature.

The relative strength of F_{ion} and F_{ch} largely depends on the charge fraction α and the grafting density σ. This paper focuses on moderately charged brushes, $\alpha \ll (l_B/a)^{-2}$, where $l_B \cong e^2/\epsilon kT$ is the Bjerrum length characterizing the strength of the Coulomb interactions (e is an elementary charge and ϵ is the dielectric constant of the solvent). In this case, F_{ion} and F_{ch} may be determined from the solution of the Poisson−Boltzmann equation for the fixed ion and free counterion densities and the electrostatic potential $\Phi(z)$ in the brush.[7,18] One can distinguish two limiting cases of moderately charged brushes. For sufficiently large α or σ, the electrostatic

screening length λ_D is much smaller than the brush thickness H. In this limit, the αN counterions per chain are essentially confined within the brush, implying its electroneutrality as a whole. For such electroneutral brushes, the counterion entropy of mixing F_{ion} is the dominant polyelectrolyte effect and the electrostatic term F_{ch} may be neglected. On the other hand, for sufficently small α or σ, the electrostatic screening length λ_D is much larger than the brush thickness. In this limit, most of the counterions are free to leave the brush, resulting in an electric double layer of thickness $\lambda_D \gg H$. In this double-layer regime, the counterion entropy of mixing plays no role and hence the electrostatic term F_{ch} is important. In the absence of flow, $\alpha_c \simeq (N^2\sigma l_B/a)^{-2/3}$ is the characteristic charge fraction separating the electroneutral and double-layer regimes.[7,18] In the electroneutral regime, the polyelectrolyte effects in the brush are expected to be strong, and hence this paper will focus on this case. However, for the sake of completeness, the double-layer regime is also discussed briefly below.

2.1. Electroneutral Regime. In the electroneutrality limit, $\lambda_D \ll H$, the counterions are localized to within a distance λ_D from the fixed ions of the polyelectrolyte chains. Thus, the average counterion volume fraction ϕ_{co} follows the fixed ion volume fraction $\alpha\phi$, except in a thin boundary layer of thickness $\lambda_D \sim a(a/\alpha^{1/2}\sigma l_B)^{1/2}$ at the free surface of the brush. The counterion term F_{ion} may be estimated from the entropy of mixing of a gas of counterions which, in the electroneutrality limit, is constrained to remain within the brush. The αN counterions per chain distributed freely in a volume $V \simeq \xi_0^2 H$ leads to a counterion entropy of mixing contribution F_{ion} per chain

$$\frac{F_{ion}}{k_B T} = \alpha N \log[\alpha\phi] \tag{3}$$

On the other hand, the direct electrostatic term F_{ch} is determined by the electrostatic energy stored in the boundary layer: $F_{ch} \simeq -\alpha N\lambda_D/H$. Since $\lambda_D \ll H$, F_{ch} may be neglected in favor of F_{ion}. Thus, the total free energy per chain F is approximately given by the sum of eqs 1−3 as

$$\frac{F}{k_B T} \simeq N\left[-\frac{1}{2}u\tau\phi + \frac{1}{6}w\phi^2 + \alpha \log[\alpha\phi] + \frac{1}{2}\sigma^2\phi^{-2}\right] \tag{4}$$

where $H = Na^3/(\phi\xi_0^2)$ has been used to write eq 1 in terms of ϕ. The numerical prefactors in eqs 1−4, unknown but assumed to be on the order of unity, have been chosen to conform to the conventions of ref 18. This form of the free energy per chain has been used previously to analyze the conformational phase behavior of Alexander−deGennes polyelectrolyte brushes in quiescent poor solvents,[17,18] the results of which are summarized in Figure 2 for the case of $\sigma = 10^{-2}$ and $u = w = 1$. In the $\alpha-\tau$ plane, there are three regions: an expanded region for relatively large α, in which counterion entropy competes with polymer elasticity ["polyelectrolyte region"; $H \sim \alpha^{1/2}Na$]; a collapsed region for relatively small α and large τ, corresponding to the usual poor solvent behavior of neutral brushes ["excluded volume region"; $H \sim (w\sigma/u\tau)Na$]; and a Θ-solvent region at relatively small α and τ, in which repulsive three-body interactions balance polymer elasticity ["Θ region"; $H \sim w^{1/4}\sigma^{1/2}Na$]. The polyelectrolyte and excluded volume regions are separated by a line of first-order stretch−collapse transitions terminating at a second-order critical point $\{\alpha_*,\tau_*\}$, with $\alpha_* \sim \sigma$ and $\tau_* \sim \sigma^{1/2}$.[18]

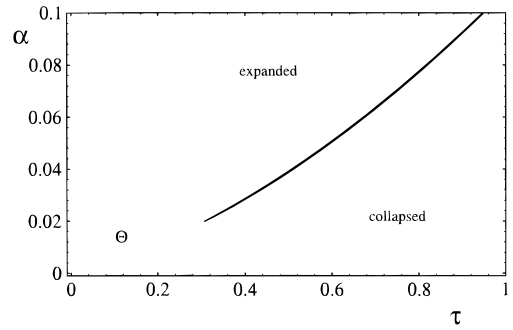

Figure 2. Plot of the phase behavior of a quiescent Alexander−deGennes polyelectrolyte brush in the electroneutral regime as a function of the charge fraction α and the reduced temperature shift τ. In the $\alpha-\tau$ plane, there are three regions: an expanded polyelectrolyte region, a collapsed excluded volume region, and a Θ-solvent region. The polyelectrolyte and excluded volume regions are separated by a line of first-order stretch−collapse transitions terminating at a second-order critical point.

The presence of permeation flow is expected to modify this phase diagram. Solvent flowing with velocity $\vec{V} = +V\hat{z}$ out of the brush should stabilize the expanded polyelectrolyte region, while solvent flowing with velocity $\vec{V} = -V\hat{z}$ into the brush should favor the collapsed state. In order to model these phenomena, one must include the effects of solvent drag in the above formalism. I do this by adding an effective work term to the total free energy and then minimizing the resulting pseudo-potential. If $f(H)$ is the total drag force per polymer chain due to solvent flow through the brush, then the resulting pseudo-potential is $G = F + F_{drag}$, where $F_{drag} = -\int f(H)\, dH$. This procedure is valid as long as one can write the drag force per polymer chain as a function of H. The total drag per chain f has two contributions: the bare drag f_p between a polymer chain and the solvent and the induced drag f_{co} due to the friction between the counterions and the solvent. The precise form of these two drag contributions depends on the details of the solvent/monomer and solvent/counterion hydrodynamic interactions and on the electrokinetic effects governing the response of the counterions to flow. A detailed discussion of these effects is beyond the scope of this work; simple scaling estimates will be used in this paper in order to illustrate some of the essential features of these drag forces. Below, I discuss the counterion contribution before the polymer−solvent contribution.

In the absence of solvent flow and external sources of counterions or salt, the counterions are essentially confined within the brush in the electroneutral regime. Solvent flow induces drag forces on the counterions, which are partially compensated by electrostatic and possible entropic restoring forces. Sufficiently strong flows can lead to a relative displacement of the counterion cloud and the grafted polyions. In particular, such behavior is possible for flow rates above $V_* \sim k_B T/(\eta\lambda_D a)$. However, in the electroneutral regime, $\lambda_D \ll H$, V_* is very large compared with typical experimental flow rates. Hence the counterions are slaved to the chains by electrostatic forces, $\phi_{co} \simeq \alpha\phi$, and the solvent drag on the trapped counterions is essentially transfered to the chains for realistic flow rates . This is the origin of the induced drag f_{co}.

In principle, long-range hydrodynamic interactions between counterions must be taken into account when

analyzing their response to solvent flow. However, since the counterions are very dilute in the grafted layer and (unlike the monomers) physically unconnected, the counterion contribution to lowest order may be approximated by the total drag on a collection of independent Stokes spheres; i.e., hydrodynamic interactions *between* the counterions may be neglected. This neglect of hydrodynamic interactions is well established for colloidal suspensions at low volume fractions.[45] Furthermore, the qualitative results of the analysis are not sensitive to this approximation. Thus, the counterion contribution to the drag per chain scales as $f_{co} \sim (\eta V b)(\alpha N)$, where b is the effective stokes radius of a counterion. For simplicity, this paper assumes $b \simeq a$.[46] Note that in the presence of a source of counterions, this counterion drag force would be substantially suppressed. Both limits may be captured in an expression of the form

$$f_{co} = c\eta V \alpha N a \tag{5}$$

where c is a coupling constant that varies from zero to a number of order unity as the counterion drag mechanism becomes relevant (comparative results in the limits of $c = 0$ and $c = 1$ are presented below).

The bare polymer contribution f_p to the drag depends on the state of the brush. In the extended polyelectrolyte region, the chains are sufficiently stretched that they can be viewed as isolated strings of hydrodynamic Zimm−Stokes blobs, for which the polymer-solvent drag per chain scales as $f_p \sim \eta V H$.[42,43] However, when the brush is in the collapsed state, it should be viewed locally as a concentrated polymer solution. In this collapsed limit, it is natural to model the polymer−solvent drag in terms of solvent friction in a porous media.[32,42] In such an approach, the drag per unit volume scales as $\eta V/\xi^2$, where $\xi \sim a/\phi$ is the local mesh size. The corresponding drag per chain scales as $f_p \sim (H\xi_0^2)(\eta V/\xi^2)$. Since $\phi \simeq Na^3/(H\xi_0^2)$, $f_p \sim \eta V (Na^2/\xi_0)^2 H^{-1}$ in this case. Hence, the two limiting cases are $f_p \sim \eta V H$ in the extended state and $f_p \sim \eta V (Na^2/\xi_0)^2 H^{-1}$ in the collapsed state. These two expressions coincide at $\xi = \xi_0$, but the crossover region between these two limits requires discussion. It is clear that the the actual $f_p(H)$ should be a nonmonotonic function of H:[42] the drag gets very large both for small H (tiny pores) and for large H (very long chains of blobs at fixed separation). Furthermore, since $(Na^2/\xi_0)^2 H^{-1}$ is small when H is large and vice versa, one may obtain a reasonable approximation to $f_p(H)$ for the whole range of H by simply adding the two limiting expressions for f_p, giving

$$f_p \simeq \eta V (H + (Na^2/\xi_0)^2 H^{-1}) \tag{6}$$

In the expanded state, where chains are rather stretched, the first term of eq 6 dominates; while in the collapsed state, the second term is most important. The qualitative features of the results are not sensitive to the precise form of $f_p(H)$. Hence, the crossover formula proposed in eq 6, although very approximate, is quite adequate for the purposes of this paper. Using eqs 5 and 6 for the total drag force per chain, $f(H) = f_{co} + f_p$, leads to an effective work term F_{drag} of the form

$$F_{drag} \simeq -\eta V \left(c\alpha N a H + \frac{1}{2}H^2 + \left(\frac{Na^2}{\xi_0}\right)^2 \log\left(\frac{H}{a}\right)\right) \tag{7}$$

The pseudo-potential $G = F + F_{drag}$ in the electroneutral regime obtained from eq 4 for the total free energy F per chain and eq 7 for the total effective work F_{drag} per chain due to solvent flow is given by

$$\frac{G}{k_B T N} \simeq -\frac{1}{2}\tau\phi + \frac{1}{6}\phi^2 + \alpha \log[\alpha\phi] + \nu\sigma \log\left(\frac{\phi}{N\sigma}\right) - c\nu\alpha\sigma\phi^{-1} + \frac{1}{2}(1-\nu)\sigma^2\phi^{-2} \tag{8}$$

where $\nu = V/V_0$ is a reduced solvent velocity scaled by $V_0 = k_B T/(\eta N a^2)$, the dimensionless virial coefficients, u and w, have been set to unity, and $H = Na^3/(\phi\xi_0^2)$ has been used to write eq 7 in terms of ϕ. Note that the bare polymer drag term acts to renormalize both the effective Gaussian elasticity and the effective counterion osmotic pressure (see the equation of state below below), while the ion drag contribution introduces a new term to the pseudo-potential G.

2.2. Double-Layer Regime. In the limit $\lambda_D \gg H$, most of the counterions are free to leave the brush and explore the double-layer region $z \lesssim \lambda_D \simeq a^2/(\alpha\sigma N l_B)$. In this case, the entropy of mixing per chain of the counterions within the brush, $F_{ion} \simeq \alpha N \log(l_B/a)$, is independent of the brush thickness and hence is not relevant.[20] Thus, the total free energy per chain in the double-layer regime, excluding an irrelevant additive constant, is $\tilde{F} = F_{el} + F_{int} + F_{ch}$, where F_{el} and F_{int} are given by eq 1 and 2 and F_{ch} is due to the electrostatic energy of the brush/counterion double layer. This electrostatic contribution can be estimated using a simplified "capacitor" model,[9,40] in which the grafted polyions and the counterion cloud are viewed as two oppositely charged layers, each with charge per unit area of order $\alpha N/\xi_0^2$. This results in a stretching Coulomb force per chain of order $l_B(\alpha N)^2/\xi_0^2$. The electrostatic energy per chain F_{ch} is the work done by this force in stretching the chain to a height H

$$\frac{F_{ch}}{k_B T} = -\alpha^2 N^2 \frac{l_B H}{\xi_0^{\,2}} \tag{9}$$

This result may also be obtained within a Poisson−Boltzmann approach.[18] The total free energy per extended chain $\tilde{F}$ is given by the sum of eqs 1, 2, and 9 as

$$\frac{\tilde{F}}{k_B T} \simeq N\left[-\frac{1}{2}u\tau\phi + \frac{1}{6}w\phi^2 - \delta\alpha^2 N^2\sigma^2\phi^{-1} + \frac{1}{2}\sigma^2\phi^{-2}\right] \tag{10}$$

where $\delta = l_B/a$ and $H = Na^3/(\phi\xi_0^2)$ has been used to write H in terms of ϕ. Note that, in contrast to the electroneutral regime, $\tilde{F}$ has a nonfactorizable dependence on N. In the absence of flow, this form of the free energy per chain gives rise to phase diagrams which are qualitatively similar to the quiescent poor solvent polyelectrolyte brush phase diagram in the electroneutral regime shown in Figure 2. Once again, there are three regions in the $\alpha-\tau$ plane: the previous excluded volume and Θ regions, as well as a modified polyelectrolyte region for which $H \sim \alpha^2 N^3 \sigma l_B$. The modified polyelectrolyte and excluded volume regions are separated by a line of first-order stretch−collapse transitions terminating at a second-order critical point.

In the presence of permeation flow, one must include the effects of solvent drag on the brush structure. As before, these effects are accounted for by adding an effective work term to the total free energy and then minimizing the resulting pseudo-potential. In principle,

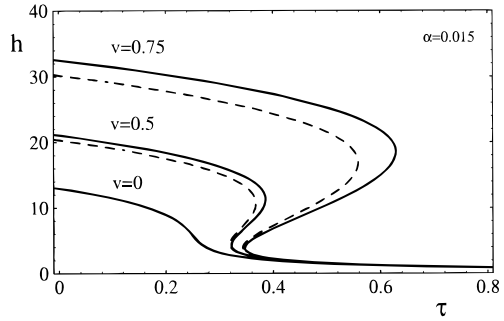

Figure 3. Plots of the electroneutral regime equation of state for $h = H/(N^{1/2}a)$ vs reduced temperature τ for $\alpha = 0.015$ and for solvent flows out of the brush. The solid curves show results with the ion drag term ($c = 1$) for $v = 0$ (bottom curve), $v = 0.5$ (middle curves), and $v = 0.75$ (top curves). The dashed curves are the analogous results without the ion drag term ($c = 0$). The solid and dashed curves coincide in the absence of flow, $v = 0$.

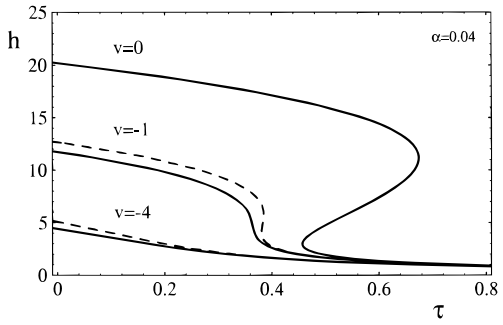

Figure 4. Plots of the electroneutral regime equation of state for $h = H/(N^{1/2}a)$ vs τ for $\alpha = 0.04$ and solvent flows into the brush with $v = 0$ (top curve), $v = -1.0$ (middle curves), and $v = -4.0$ (bottom curves). The solid curves show results with the ion drag term ($c = 1$), and the dashed curves are the analogous results without the ion drag term ($c = 0$).

the total drag per chain includes contributions from both the bare drag between polymer and solvent and the induced drag due to the friction between counterions and solvent. Furthermore, since $\lambda_D \gg H$, $V_* = k_BT/(\eta\lambda_D a)$ may lie in the range of experimental flow rates and so the flow can significantly perturb the counterion distribution in this double-layer regime. However, since the distribution of counterions in this regime plays a relatively minor role in determining brush properties, their contribution to the induced drag on the brush is much smaller than the bare polymer contribution. Hence, the effects of counterion drag may be neglected in this regime, and the effective work term F_{drag} may be approximated by eq 7 with $c = 0$. Together with eq 10 for $\tilde{F}$, this gives a pseudo-potential $\tilde{G} = \tilde{F} + F_{drag}$ of the form

$$\frac{\tilde{G}}{k_BTN} \simeq -\frac{1}{2}\tau\phi + \frac{1}{6}\phi^2 - \delta\alpha^2N^2\sigma^2\phi^{-1} + v\sigma\log\left(\frac{\phi}{N\sigma}\right) + \frac{1}{2}(1-v)\sigma^2\phi^{-2} \quad (11)$$

where $v = V/V_0$ is a reduced solvent velocity scaled by $V_0 = k_BT/(\eta Na^2)$, the dimensionless virial coefficients, u and w, have been set to unity, and $H = Na^3/(\phi\xi_0^2)$ has been used to write eq 11 in terms of ϕ. As before, the bare polymer drag term acts to renormalize the effective Gaussian elasticity and also adds an effective counterion osmotic pressure term.

3. Analysis and Results

This section presents results for the brush phase behavior under flow obtained through the analysis of the appropriate pseudo-potential. The case of brushes in the electroneutral regime is analyzed first in some detail, followed by an abbreviated analysis of the double-layer regime.

3.1. Electroneutral Regime Analysis. Using the pseudo-potential $G(\phi,v,\alpha,\tau)$ from eq 8, the equation of state in steady flow conditions is given by the solution of $\partial G/\partial\phi = 0$, which has the implicit form

$$0 = \frac{1}{3}\phi^4 - \frac{1}{2}\tau\phi^3 + (\alpha + \sigma v)\phi^2 + cv\alpha\sigma\phi + (v-1)\sigma^2 \quad (12)$$

Figure 3 shows samples of the electroneutral regime equation of state obtained from eq 12 and presented as plots of the reduced brush thickness $h = H/(N^{1/2}a)$ vs reduced temperature τ for $\alpha = 0.015$, $N = 10^4$, and $\sigma = 0.01$ and for several values of v. (All electroneutral regime examples will have $N = 10^4$ and $\sigma = 0.01$.) Note that $\alpha = 0.015$ is below the critical value α_* in the absence of flow; see Figure 2. The solid curves in Figure 3 show results with the ion drag term ($c = 1$) for $v = 0$ (bottom curve), $v = 0.5$, and $v = 0.75$ (top curve). The dashed curves are the analogous results without the ion drag term ($c = 0$). Note that the solid and dashed curves coincide in the absence of flow, $v = 0$. The plot of h vs τ for a quiescent brush ($v = 0$) indicates a smooth, continuous change of brush thickness with solvent quality. However, the plots with $v > 0$ show an emerging van der Waals loop indicative of a mean-field first-order expanded−collapsed transition. In the loop region, there is a discontinuous jump between the lower and upper branches of the equation of state in response to a change in τ. Thus, a flow of solvent outward normal to the brush can destabilize the brush-swelling behavior. This is in agreement with results for the behavior of an externally perturbed neutral polymer brush under poor solvent conditions:[47] the neutral brush collapse transition becomes first-order in response to a stretching force applied to the free chain ends, provided that the force does not decrease too rapidly with H. Note also that the jump Δh of brush thickness at the transition increases with increasing V. This is because the height of the brush in the collapsed excluded volume region is essentially independent of V, whereas the height in the expanded polyelectrolyte region is an increasing function of V. In the absence of the ion drag term ($c = 0$), this expanded brush height scales as $H \sim \alpha^{1/2}(1-v)^{-1/2}Na$. The dependence of H on V is somewhat stronger when ion drag is included; however, there are no simple scaling relations in this case.

Figure 4 shows analogous equations of state for $\alpha = 0.04$ and for $v = 0$ (top curve), $v = -1.0$ (middle curves), and $v = -4.0$ (bottom curves). Note that $\alpha = 0.04$ is above the critical value α_* in the absence of flow; see Figure 2. In this case, an unstable quiescent brush ($v = 0$) is stabilized by a sufficiently large solvent flow rate *into* the brush ($v < 0$). One can also examine the swelling behavior as a function of solvent velocity at fixed charge fraction α and temperature τ. Figure 5 shows plots of $h = H/(N^{1/2}a)$ vs the reduced solvent velocity v for $\alpha = 0.04$ and for $\tau = 0.25$, 0.35, and 0.45. Both the solid ($c = 1$) and dashed ($c = 0$) curves show the same qualitative behavior: For $\tau = 0.25$ and 0.35, the brush height varies smoothly with v, while for $\tau = 0.45$ there is a first-order stretch−collapse transition as a function of flow rate.

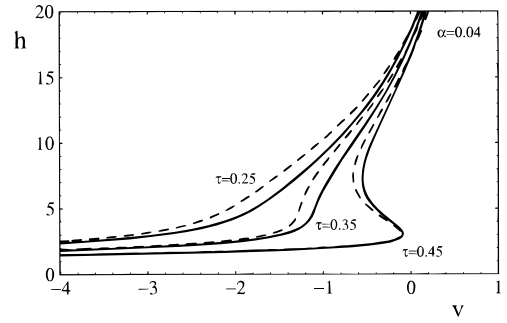

Figure 5. Plots of the electroneutral regime equation of state for $h = H/(N^{1/2}a)$ vs the reduced solvent velocity v for $\alpha = 0.04$ and for $\tau = 0.25$, 0.35, and 0.45. The solid curves are results with the ion drag term ($c = 1$), and the dashed curves are the analogous results without the ion drag term ($c = 0$).

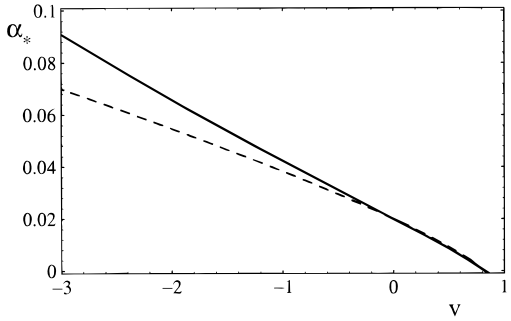

Figure 6. Plots of the critical charge fraction α_* vs v in the electroneutral regime. The solid curves are results with the ion drag term ($c = 1$), and the dashed curves are the analogous results without the ion drag term ($c = 0$).

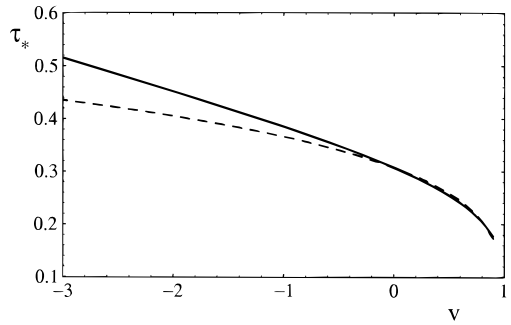

Figure 7. Plots of the critical reduced temperature τ_* vs v in the electroneutral regime. The solid curves are results with the ion drag term ($c = 1$), and the dashed curves are the analogous results without the ion drag term ($c = 0$).

The spinodal curve is obtained from the solution of $\partial^2 G/\partial\phi^2 = 0$, which may be written as

$$\alpha(\phi_s) = \left(\frac{1}{3}{\phi_s}^4 - v\sigma{\phi_s}^2 + 3(1-v)\sigma^2\right)/({\phi_s}^2 + 2cv\sigma\phi_s) \quad (13)$$

Notice that the spinodal curve $\alpha(\phi_s)$ has no explicit τ dependence. Equation 13 gives the critical volume fraction ϕ_* as the solution of $(\partial\alpha(\phi_s)/\partial\phi_s)|\phi_* = 0$, which has the form

$$0 = {\phi_*}^5 + 3cv\sigma{\phi_*}^4 - 3cv^2\sigma^2{\phi_*}^2 + 9(v-1)\sigma^2\phi_* + 9c(v-1)v\sigma^3 \quad (14)$$

For a given value of v, eqs 12−14 give the critical point $\{\alpha_*(v),\tau_*(v)\}$. Figure 6 shows plots of α_* vs v, while Figure 7 shows τ_* vs v. Once again, the solid line result includes the ion drag term, and the dashed line does not. These plots show that the ion drag term plays a more significant role in determining the critical point for $v < 0$, in which case the brush is relatively dense. The scaling of the critical point with v is nontrivial in the presence of the ion-drag term (solid curves) but rather simple in its absence: τ_* and α_* can be obtained from the quiescent solvent results of ref 18 given in the previous section by shifting the charge fraction, $\alpha \rightarrow \alpha + \sigma v$, and rescaling the grafting density, $\sigma \rightarrow \sigma(1-v)^{1/2}$. Thus, $\alpha_* \sim \sigma(1-v)^{3/2}$ and $\tau_* \sim \sigma^{1/2}(1-v)^{1/4}$ for $c = 0$. Note that the analysis given above breaks down at $v = 1$: for $v \gtrsim 1$, the thickness of the expanded phase diverges. This breakdown occurs because the finite extensibility of chains is not taken into account in the present model (cf. eq 1). Qualitatively, the trend toward decreasing α_* with increasing v is due to the rescaling of the effective Gaussian elasticity and the increase of the effective charge fraction with v, while the trend toward decreasing τ_* with increasing v is caused by the implicit dependence of the effective grafting density σ on v due to the rescaling of the effective Gaussian elasticity in solvent flow.

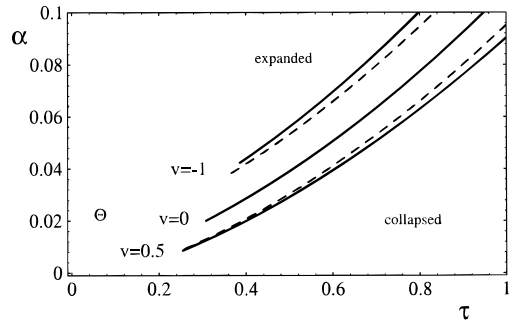

Figure 8. Flow-modified phase behavior of an electroneutral regime Alexander−deGennes polyelectrolyte brush in solvent permeation flows as a function of the charge fraction α and the reduced temperature τ. The middle solid curve is the quiescent transition line ($v = 0$) shown in Figure 2. The upper pair of curves are for $v = -1.0$, while the lower pair are for $v = 0.5$. The solid curves show results with the ion drag term ($c = 1$), and the dashed curves are the analogous results without the ion drag term ($c = 0$).

One can obtain the first-order transition line numerically by finding the locus of pairs along the equation of state, eq. 12, which have equal values of G (the slope of the common tangent is zero in this case). This procedure gives a line of first-order stretch−collapse transitions $\alpha_t(\tau)$ for each value of the reduced solvent velocity v. This transition line terminates at the second-order critical point discussed above and plotted in Figures 6 and 7. Thus, the flow does not change the first-order nature of the stretch−collapse transition within an Alexander−deGennes treatment, although the location the transition line is sensitive to the flow. Figure 8 shows sample plots of these transition lines, both with and without the ion drag term. The middle solid curve is the quiescent transition line ($v = 0$) shown in Figure 2. The upper pair of curves are for $v = -1.0$, while the lower pair are for $v = 0.5$. As with the critical point, the flow shifts the transition line toward smaller τ and α for $v > 0$ and toward larger τ and α for $v < 0$. These shifts are larger when the extra drag due to the counterions is accounted for (solid lines).

3.2. Double-Layer Regime Analysis. The analysis of the double-layer regime closely follows the procedure described for the electroneutral regime above. Using the pseudo-potential $\tilde{G}(\phi,v,\alpha,\tau)$ from eq 11, the equation

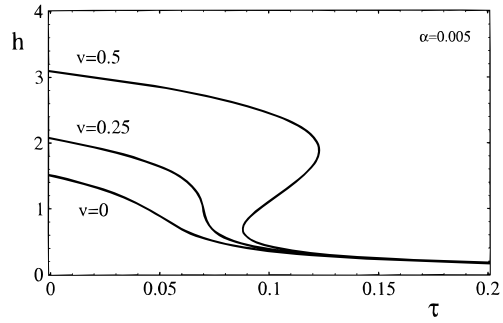

Figure 9. Plots of the double-layer regime equation of state for $h = H/(N^{1/2}a)$ vs τ for $\alpha = 0.005$ and for solvent flows out of the brush. The curves show results for $v = 0$ (bottom curve), $v = 0.25$ (middle curve), and $v = 0.5$ (top curve).

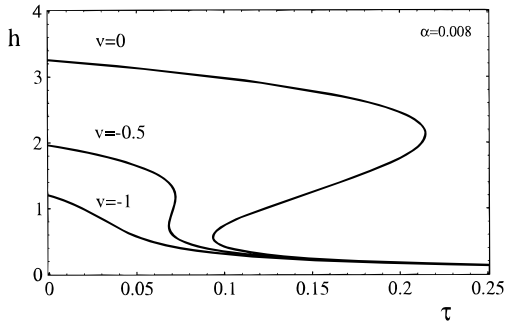

Figure 10. Plots of the double-layer regime equation of state for $h = H/(N^{1/2}a)$ vs reduced τ for $\alpha = 0.008$ and solvent flows into the brush with $v = 0$ (top curve), $v = -0.5$ (middle curve), and $v = -1.0$ (bottom curve).

of state in steady flow conditions, obtained from $\partial\tilde{G}/\partial\phi = 0$, is given by the solution of

$$0 = \frac{1}{3}\phi^4 - \frac{1}{2}\tau\phi^3 + v\sigma\phi^2 + \delta\alpha^2\sigma^2N^2\phi + (v-1)\sigma^2 \quad (15)$$

Figure 9 shows samples of the double-layer regime equation of state obtained from eq 15 and presented as plots of the reduced brush thickness $h = H/(N^{1/2}a)$ vs reduced temperature τ for $\alpha = 0.005$, $N = 10^3$, $\sigma = 0.0016$, $\delta = 1$ and for $v = 0$ (bottom curve), $v = 0.25$, and $v = 0.5$ (top curve). (All double-layer regime examples will have $N = 10^3$, $\sigma = 0.0016$, and $\delta = 1$.) While the plot of h vs τ for a quiescent brush ($v = 0$) indicates a smooth, continuous change of brush thickness with solvent quality, the plots with $v > 0$ show an emerging van der Waals loop indicative of a mean-field first-order expanded−collapsed transition. Thus, as in the electroneutral regime, a flow of solvent outward normal to the brush can destabilize the brush swelling behavior (cf. Figure 3). The jump Δh of the brush thickness at the transition increases with V due to the dependence of the expanded polyelectrolyte state on flow rate: $H \sim \alpha^2N^3\sigma l_B(1-v)^{-1}$. Figure 10 shows analogous equations of state for $\alpha = 0.008$ and for $v = 0$ (top curve), $v = -0.5$ (middle curve), and $v = -1.0$ (bottom curve). Hence, a brush which is unstable in quiescent conditions ($v = 0$) can be stabilized by a sufficiently large solvent flow rate *into* the brush ($v < 0$), as in the electroneutral regime (cf. Figure 4). Note that brushes in the double-layer regime are more sensitive to flow than in the electroneutral regime, due to the weak polyelectrolyte effects in the double-layer regime.

The spinodal curve, obtained from $\partial^2\tilde{G}/\partial\phi^2 = 0$, has the form

$$\alpha(\phi_s) = \left(\frac{1}{3}\phi_s^{\,3} - v\sigma\phi_s + 3(1-v)\sigma^2\phi_s^{\,-1}\right)^{1/2}/(\sqrt{2\delta}\sigma N) \quad (16)$$

As before, the spinodal curve $\alpha(\phi_s)$ has no explicit τ dependence. Equation 16 gives the critical volume fraction ϕ, as the solution of $(\partial\alpha(\phi_s)/\partial\phi_s)|\phi_* = 0$

$$\phi_* = \left(\frac{\sigma}{2}\right)^{1/2}[v + (v^2 - 12v + 12)^{1/2}]^{1/2} \quad (17)$$

For a given value of v, eqs 15−17 give the critical point $\{\alpha_*(v),\tau_*(v)\}$. In quiescent conditions ($v = 0$), one finds $\alpha_* \sim \sigma^{-1/4}N^{-1}$ and $\tau_* \sim \sigma^{1/2}$. At finite v, there is no simple scaling behavior. However, $\alpha_*(v)$ decreases linearly and $\tau_*(v)$ increases linearly with v in the limit $|v| \ll 1$.

The first-order transition line in the double-layer regime is obtained by finding the locus of pairs along the equation of state, eq 15, which have equal values of $\tilde{G}$. As in the electroneutral regime, this procedure gives a line of first-order stretch−collapse transitions $\alpha_t(\tau)$ for each value of the reduced solvent velocity v. This transition line terminates at the second order critical point obtained from eqs 15−17. Figure 11 shows sample plots of the transition lines in the double-layer regime. The middle curve is the quiescent transition line ($v = 0$) and is analogous to the quiescent electroneutral regime transition line shown in Figure 2. The upper curve is for $v = -1.0$, while the lower one is for $v = 0.5$. In double-layer regime, the flow shifts the transition line and the critical point toward smaller α and larger τ for $v > 0$, and toward larger α and smaller τ for $v < 0$. The shift in α with v is qualitatively similar to the behavior in the electroneutral regime and is due to the rescaling of the effective Gaussian elasticity in solvent flow. However, the shift toward larger τ with increasing v is opposite to the behavior in the electroneutral regime, although it is a rather small effect.

4. Discussion

This paper has presented a simple analysis of the effects of idealized permeation flow on the phase behavior of grafted polyelectrolyte layers in poor solvent conditions. These effects were investigated using a model based on the Alexander−deGennes ansatz that all chains behave alike in flow and the approximation of spatially uniform brush deformation. Both the electroneutrality regime (at moderate charge per unit area) and the double-layer regime (at low charge per unit area) have been analyzed. This model accounts for both the polymer-solvent drag forces and for some of the possible effects of solvent drag forces on the counterions within the brush. For the case of electroneutral brushes exposed to flows into the brush, the latter drag mechanism can play a significant role.

The results of this analysis indicate that the first-order nature of the stretch−collapse transition occurring for Alexander−deGennes polyelectrolyte brushes in quiescent poor solvents also remains in the presence of solvent flow in both regimes studied. However, there is a significant shift in the location of the first-order transition line and the second-order critical point as a function of solvent flow rate. In particular, the flow generally shifts the critical point and transition line toward smaller α for flows out of the brush and toward larger α for flows into the brush [cf. Figures 6−8 and 11]. For brushes in the electroneutral regime, the flow shifts the transition line and the critical point toward larger τ with decreasing v, whereas in double-layer

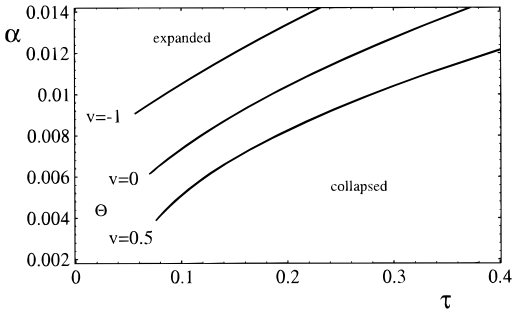

Figure 11. Flow-modified phase behavior of a double-layer regime Alexander−deGennes polyelectrolyte brush in solvent permeation flows as a function of the charge fraction α and the reduced temperature τ. The middle solid curve is the quiescent transition line ($v = 0$). The upper curve is for $v = -1.0$, while the lower is for $v = 0.5$.

regime these shifts are toward slightly smaller τ with decreasing v. Qualitatively, this difference can be understood as follows. In the double-layer regime, the electrostatic contribution to the force on a chain is independent of H. Thus, with decreasing flow rate there is an increased preference for brush collapse which is not compensated by electrostatic forces, and hence there is a decreasing τ_* with decreasing v. Whereas in the electroneutral regime, corresponding to brushes with relatively high charge per unit area, the tendency toward collapse with decreasing v is counteracted by a counterion osmotic pressure that strongly increases with decreasing H. As well as modifying the location of the transition, solvent flow also changes the susceptibility the brush: the discontinuity in brush thickness across the phase boundary is an increasing function of solvent flow rate. Moreover, brushes in the double-layer regime are more sensitive to flow than in the electroneutral regime, due to the weak polyelectrolyte effects in this regime (compare Figures 3 and 4 with Figures 9 and 10).

The approach described here has several inherent limitations. The principal assumption, the Alexander−deGennes ansatz that all chains stretch alike, is violated for both neutral[12,13] and charged[5,6,8,10] polymer brushes under equilibrium conditions.[48] For polyelectolyte brushes in quiescent poor solvents, there is also the possibility of internal structural inhomogeneity, either due to lateral[20] or layer-wise[25,26] microphase separation within the brush. It should be noted that the effects of structural inhomogeneities and fluctuations in the positions of free chain ends in a polyelectolyte brush on the nature of the collapse behavior in quiescent conditions is still unclear.[18,19,26] Although not directly addressed in this work, one might expect that external forces, such as the hydrodynamic drag due to solvent flow, would somewhat suppress structural inhomogeneities, leading to a more uniform brush structure in steady-state flow conditions. It may also happen that solvent flow through the brush will favor a particular type of structural inhomogeneity. For instance, in the presence of the permeation flows discussed in this work, one might expect laterally inhomogeneous brushes[20−24] to be selected over layer-wise phase-separated brushes.[26] The question of the coupling of flow to structural heterogeneity and its effects on phase behavior is a very interesting and important subject for future studies.

The present analysis considers a rather idealized flow geometry, uniform permeation flow normal to the grafted layer, and a simplified treatment of hydrodynamic interactions and electrokinetic effects. In particular, the hydrodynamic interactions between counterions and the effects of the relative shift of the polylelectrolyte and counterion concentrations, ϕ and ϕ_{co}, as a function of flow rate were neglected. The neglect of counterion hydrodynamic interactions is reasonable as long as the volume fraction of counterions is sufficiently low, $\phi_{co} \ll 1$. The neglect of the relative shift of ϕ and ϕ_{co} with V is valid in the electroneutral regime (in which the characteristic flow rate V_* for this effect is very large) and in the double-layer regime (in which counterion drag plays a very weak role in any case). However, this effect may alter brush phase behavior in the crossover regime at intermediate charge densities. The model presented here is particularly suited for uniform permeation flow conditions, since it admits a description in terms of a potential. Although these flows are rather idealized, the qualitative trends predicted may also occur in more realistic flows. For instance, there is the possibility of flow-induced flocculation of polyelectrolyte-coated colloids in marginally poor solvent conditions due to the collapse of the grafted polyelectrolyte layers in squeezing flow situations. Flow-induced collapse phenomena might also occur for polyelectolytes grafted to porous membrane materials subjected to permeation flows, resulting in modified membrane permeability. It should be noted that realistic permeation flows are somewhat inhomogeneous, especially near the grafting surface. Nevertheless, the idealized flows considered in this paper provide a relatively clean and simple foundation for future studies of more realistic flows. In order to address the effects of more general flows on poor solvent polyelectrolyte brushes, it may be necessary to resort to an approach involving local force balance within the brush, such as that used to analyze the deformation of polymer brushes in flows of good solvent.[37,40,42] The effects of shear flows on the phase behavior of polyelectrolyte brushes in poor solvents is a particularly interesting problem under current investigation. Finally, a more detailed analysis of hydrodynamic interactions and electrokinetic effects, and of the resulting steady-state response of counterions within and outside of the brush may be required in some situations.

Acknowledgment. It is a pleasure to thank O. V. Borisov and M. E. Cates for very stimulating comments and discussions, and G. Porte for hospitality during an extended visit in the Groupe de Dynamique des Phases Condensées at the Université Montpellier II. This work was supported in part by the CNRS Poste Rouge program.

References and Notes

(1) Milner, S. T. *Science* **1991**, *251*, 905.
(2) Halperin, A.; Tirrell, M.; Lodge, T. P. *Adv. Polym. Sci.* **1992**, *100*, 33.
(3) Szleifer, I.; Carignano, M. A. *Adv. Chem. Phys.* **1996**, *94*, 165.
(4) Barrat, J.-L.; Joanny, J.-F. *Adv. Chem. Phys.* **1996**, *94*, 1.
(5) Miklavic, S. J.; Marcelja, S. *J. Phys. Chem.* **1988**, *92*, 6718.
(6) Misra, S.; Varanasi, S.; Varanasi, P. P. *Macromolecules* **1989**, *22*, 4173.
(7) Pincus, P. *Macromolecules* **1991**, *24*, 2912.
(8) Zhulina, E. B; Borisov, O. V.; Birshtein, T. M. *J. Phys. II Fr.* **1992**, *2*, 63.
(9) Borisov, O. V., Zhulina, E. B., Birshtein, T. M. *Macromolecules* **1994**, *27*, 4795.
(10) Von Goeler, F.; Muthukumar, M. *Macromolecules* **1995**, *28*, 6608.
(11) Hirz, S. Modeling of Interactions Between Adsorbed Block Copolymers. M.S. Thesis, University of Minnesota, Minneapolis, MN, 1988.

(12) Milner, S. T.; Witten, T. A.; Cates, M. E. *Europhys. Lett.* **1988**, *5*, 413; *Macromolecules* **1988**, *21*, 2610.
(13) Skvortsov, A. M.; Gorbunov, A. A.; Pavlushkov, I. V.; Zhulina, E. B.; Borisov, O. V.; Priamitsyn, V. A. *Polym. Sci. USSR* (*Engl. Transl.*) **1988**, *30*, 1706.
(14) Borisov, O. V.; Zhulina, E. B.; Birshtein, T. M. *Poly. Sci. USSR* (*Engl. Transl.*) **1988**, *30*, 772; Zhulina, E. B.; Borisov, O. V.; Pryamitsyn, V. A. *J. Colloid Interface Sci.* **1990**, *137*, 495.
(15) Alexander, S. *J. Phys. Paris* **1977**, *38*, 983.
(16) De Gennes, P. G. *J. Phys. Paris* **1976**, *37*, 1443; *Macromolecules* **1980**, *13*, 1069.
(17) Borisov, O. V.; Birshtein, T. M.; Zhulina, E. B *J. Phys. II Fr.* **1991**, *1*, 521.
(18) Ross, R. S.; Pincus, P. *Macromolecules* **1992**, *25*, 2177.
(19) Von Goeler, F.; Muthukumar, M. *J. Chem. Phys.* **1996**, *105*, 11335.
(20) Ross, R. S. Structural Order in Two Complex Fluid Systems. Ph.D. Thesis, University of California, Santa Barbara, CA, 1993.
(21) Yeung, C.; Balazs, A. C.; Jasnow, D. *Macromolecules* **1993**, *26*, 1914.
(22) Williams, D. R. M. *J. Phys. Fr. II* **1993**, *3*, 1313.
(23) Tang, H.; Szleifer, I. *Europhys. Lett.* **1994**, *28*, 19.
(24) Zhulina, E. B.; Birshtein, T. M.; Priamitsyn, V. A.; Klushin, L. I. *Macromolecules* **1995**, *28*, 8612.
(25) Misra, S.; Mattice, W. L.; Napper, D. H. *Macromolecules* **1994**, *27*, 7090.
(26) Misra, S.; Tirrell, M. V.; Mattice, W. L. *Macromolecules* **1996**, *29*, 6056.
(27) Borue, V. Yu.; Erukhimovich, I. Ya. *Macromolecules* **1988**, *21*, 3240.
(28) Joanny, J.-F.; Leibler, L. *J. Phys. Paris* **1990**, *51*, 545.
(29) Klein, J.; Perahia, D.; Warburg, S. *Nature* **1991**, *352*, 143.
(30) Klein, J. *Annu. Rev. Mater. Sci.* **1996**, *26*, 581.
(31) Klein, J.; Kamiyama, Y.; Yoshizawa, H.; Israelachvili, J. N; Fredrickson, G. H.; Pincus, P; Fetters, L. J. *Macromolecules* **1993**, *26*, 5552.
(32) Fredrickson, G. H.; Pincus, P. *Langmuir* **1991**, *7*, 786.
(33) Milner, S. T. *Macromolecules* **1991**, *24*, 3704.
(34) Rabin, Y.; Alexander, S. *Europhys. Lett.* **1990**, *13*, 49.
(35) Barrat, J.-L. *Macromolecules* **1992**, *25*, 832.
(36) Kumaran, V. *Macromolecules* **1993**, *26*, 2464.
(37) Harden, J. L.; Cates, M. E. *Phys. Rev. E* **1996**, *53*, 3782.
(38) Aubouy, M.; Harden, J. L.; Cates, M. E. *J. Phys. II Fr.* **1996**, *6*, 969.
(39) Birshtein, T. M.; Zhulina, E. B. *Makromol. Chem., Theory Simul.* **1992**, *1*, 193.
(40) Harden, J. L.; Borisov, O. V.; Cates, M. E.; *Macromolecules* **1997**, *30*, 1179.
(41) Williams, D. R. M *Macromolecules* **1993**, *26*, 5808.
(42) Harden, J. L.; Cates, M. E. J. Phys. II France, **1995**, *5*, 1093; Erratum *Ibid*. **1995**, *5*, 1757.
(43) Brochard-Wyart, F. *Europhys. Lett.* **1993**, *23*, 105; Brochard-Wyart, F.; Hervet, H.; Pincus, P. *Europhys. Lett.* **1994**, *26*, 511.
(44) Zhulina, E. B.; Birshtein, T. M.; Borisov, O. V. *Macromolecules* **1995**, *28*, 1491.
(45) Russel, W. B.; Saville, D. A.; Schowalter, W. R. *Colloidal Dispersions*; Cambridge University Press: Cambridge, England, 1991.
(46) The effective Stokes radius of a counterion is the sum of the bare ion size and the thickness of the hydration shell around it. The bare ion size may be much smaller than *a*, but the thickness of the hydration shell can be substantial.
(47) Halperin, A.; Zhulina, E. B. *Macromolecules* **1991**, *29*, 5393.
(48) Note that these fluctuations become less pronounced in the collapsed state of a brush under poor solvent conditions.

MA961856K